COMMUNICATIONS

Complete kinematic measurement of three-body reaction dynamics: Dissociative photodetachment of O_6^- at 532 nm

K. A. Hanold,[a] A. K. Luong, and R. E. Continetti
Department of Chemistry and Biochemistry, 0314, University of California, San Diego, 9500 Gilman Drive, La Jolla, California 92093-0314

(Received 1 September 1998; accepted 25 September 1998)

Measurement of the translational energy partitioning in the three-body dissociative photodetachment of O_6^- ($O_6^- + h\nu \rightarrow O_2 + O_2 + O_2 + e^-$) at 532 nm is reported. Using photoelectron and photofragment translational energy spectroscopies in coincidence, a complete kinematic measurement of the three-body dissociation of neutral O_6 is obtained. Vibrationally resolved product translational energy distributions are observed. The results provide insights into the structure, binding energy, and dissociation dynamics of O_6^- and O_6 and illustrate a new approach to the study of three-body reaction dynamics. © *1998 American Institute of Physics.* [S0021-9606(98)02745-7]

In recent years, there has been an increased interest in developing a more detailed experimental and theoretical understanding of three-body chemical reactions.[1,2] Significant experimental progress has been made in studies of the dissociation of multiply charged cations and other high energy systems.[3–5] Detailed experimental studies of the dynamics of three-body reactions of neutral species, however, have been limited to excited-state photodissociation reactions leading to either prompt or sequential dissociation processes. These experiments have in general relied on measurements of the uncorrelated asymptotic properties of the photofragments such as momentum and quantum state.[1,6–11] The overall three-body dynamics has then been inferred from the data using theoretical guidance to determine the forces at the transition state for dissociation. In our laboratory, we have sought to develop a technique to study three-body dissociation processes on the electronic ground state for neutral systems. The approach we have taken is one developed in our laboratory and previously applied to two-body dissociation processes, photoelectron–photofragment coincidence spectroscopy.[12] In these experiments, photodetachment of a precursor negative ion and energy analysis of the photoelectron is used to prepare a neutral complex with a known internal energy that subsequently dissociates. Use of a fast precursor negative-ion beam and a new multiparticle detector allows collection of the three photofragments in coincidence, providing a direct measure of the translational energy and angular distributions of the photofragments in a three-body dissociation.

In this communication, we describe the application of this technique to the study of the three-body dissociation reaction initiated by dissociative photodetachment (DPD) of the O_6^- cluster anion. Photodetachment of anions can produce a neutral complex far from the equilibrium geometry, and the repulsive energy in the cluster can lead to a rapid dissociation. To determine the energetics and dissociation dynamics of such short lived neutral clusters, a measurement of the photoelectron kinetic energy alone is insufficient—it is necessary to measure the photoelectron kinetic energy in *coincidence* with the translational energy release.[12]

The homogeneous cluster anions of O_2, of which O_4^- and O_6^- are the simplest, are known to exhibit a rich photochemistry, undergoing both photodissociation and photodetachment with visible photons.[13,14] In the case of O_4^-, energetic considerations indicate that at 532 nm (2.33 eV), DPD produces a free electron and two ground state O_2 ($^3\Sigma_g^-$) molecules. Mass spectrometric studies have shown that O_6^- is stabilized relative to O_4^- by 0.11 eV,[15] thus DPD of O_6^- at 532 nm will yield a free electron and three ground state O_2 molecules. Recent work on O_4^-, both in gas-phase[16,17] and matrix isolation[18] studies, has indicated that the excess electron is delocalized over both O_2 moieties in a planar D_{2h} structure with a ^2A_u electronic ground state. In a previous study of O_6^-, Johnson and co-workers[13] observed a significant enhancement of photodissociation at long wavelengths (1064 nm) relative to O_4^-. It has been suggested that this is due to a charge-transfer-to-solvent interaction between an O_4^- core and the ''solvating'' O_2.[13] The present experiments focus on the DPD of O_6^- at 532 nm, and as shown below, reveal a vibrationally resolved translational energy distribution as well as new photodissociation channels unobserved in O_4^-.

A schematic of the detection geometry is shown in Fig. 1. The photoelectron–photofragment spectrometer is described in detail elsewhere[19] and will only be briefly described here. Anions are made and cooled in a pulsed free jet expansion of O_2 intersected by a 1 keV electron beam. The anions are accelerated to an energy of 4 keV and mass selected by time of flight. Anions at $m/e = 96$ are intersected

[a]Present address: Syagen Technology, Inc., 1411 Warner Ave., Suite B, Tustin, CA 92780.

by a 120 μJ/pulse, 100 ps full width at half-maximum (FWHM), linearly polarized 532 nm laser beam.[20] In these experiments, the electric vector of the laser was fixed parallel to the ion beam direction. Photoelectrons traverse a nominal 50 mm field-free flight path and impinge on one of two 100-mm-diam detectors, both centered perpendicular to the laser electric vector on opposite sides of the ion beam. The two time- and position-sensitive photoelectron detectors comprise the photoelectron spectrometer and have an effective angular acceptance of 21% of 4π sr. Using the time and position information, the electron recoil angle and actual flight path are calculated, allowing correction for the large Doppler shift associated with the ion beam as a function of angle. The center-of-mass electron kinetic energy (eKE) resolution is $\Delta E/E$ (FWHM)=5% at 1.3 eV as determined by measurements of the O_2^- photoelectron spectrum at 532 nm.

Photofragments recoil out of the beam over a 104 cm flight path between the laser interaction region and the photofragment detector. Residual ions and ionic photofragments are electrostatically deflected away from the detector. The photofragment detector consists of four quadrants, each capable of recording the time and position of arrival of up to two photofragments. This microchannel-plate-based detector uses a crossed delay-line format for the anode,[21,22] with each delay line instrumented to record two photofragments per shot as long as they are separated by a delay-line length of $\approx$25 ns. There is effectively no dead area within the 40 mm active diameter of this detector, since an event arriving on a quadrant boundary will excite two quadrants, and can be subsequently analyzed and assigned to one of them by an analysis of the event charge. The time and position of arrival of the photofragments together with conservation of momentum determine the recoil angles, photofragment mass ratios, and the total center-of-mass translational energy release (E_T) for the three molecular photofragments. Due to the small recoil of one of the O_2 products in the case of O_6^-, the product mass resolution of the apparatus is low ($m/\Delta m \approx 2$). Energetic considerations, however, dictate that three-body DPD processes for O_6^- at this wavelength must yield $3O_2+e^-$. The translation energy resolution of the apparatus is $<$8% $\Delta E/E$ at 0.8 eV, as determine by studies of the photodissociation of O_4^- at 532 nm.[14] The angular acceptance is a full circle covering 100% of 4π sr given the beam energy and the kinematics of this reaction.

Each event is required to consist of a single electron and three neutral photofragments. Conservation of momentum allows discrimination against false photofragment coincidences while correlation of the electron and photofragments is determined by the spectrometer efficiency and the count rate. These experiments were carried out at repetition rate of 500 Hz and the observed quadrupole coincidence rate of 0.1 Hz yields $\approx$5% false coincidences.

The O_6^- data at 532 nm have been analyzed for both two- and three-body dissociation pathways, and the only dissociation pathway observed is $O_6^- + h\nu \rightarrow 3O_2(^3\Sigma_g^-) + e^-$. This is in accord with our studies of O_4^-, which show that no stable O_4 is produced. To examine the partitioning of translational energy among the photoelectron and the three

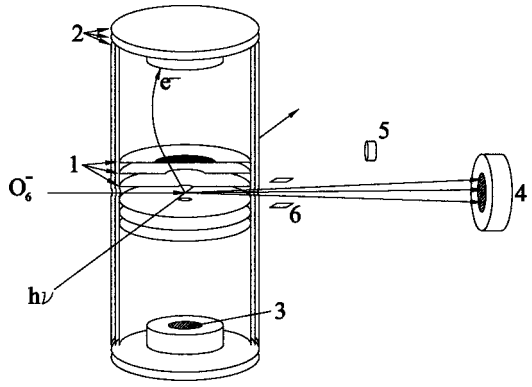

FIG. 1. Schematic of the experimental geometry for the detection of $O_2+O_2+O_2+e^-$, showing the orientation of the O_6^- ion beam, the laser beam, and the particle detectors. The numbered components are as follows: (1) photoelectron spectrometer apertures, (2) mu-metal magnetic shielding, (3) photoelectron detectors, (4) multiparticle photofragment detector, (5) undetached ion detector, (6) ion beam deflector.

photofragments produced in the DPD of O_6^-, it is useful to examine the photoelectron–photofragment correlation spectra, $N(\text{eKE}, E_T)$, as shown in Fig 2. This shows a two-dimensional histogram of the correlation between eKE and E_T. The spectra along the eKE and E_T axes are found by integrating over the complementary variable and are the photoelectron and photofragment translational energy release spectra that are measurable in conventional noncoincidence spectrometers. The limit *A* corresponds to the maximum kinetic energy among the four particles ($3O_2+e^-$), given the 0.11 eV stability of O_6^- relative to $O_4^-+O_2$ inferred from these experiments and mass spectrometric studies by Hiraoka.[15]

The dominant feature observed in Fig. 2 arises from the three-body DPD process $[O_6^- + h\nu \rightarrow 3O(X\ ^3\Sigma_g^-) + e^-]$. This pathway appears as the series of diagonal ridges marked

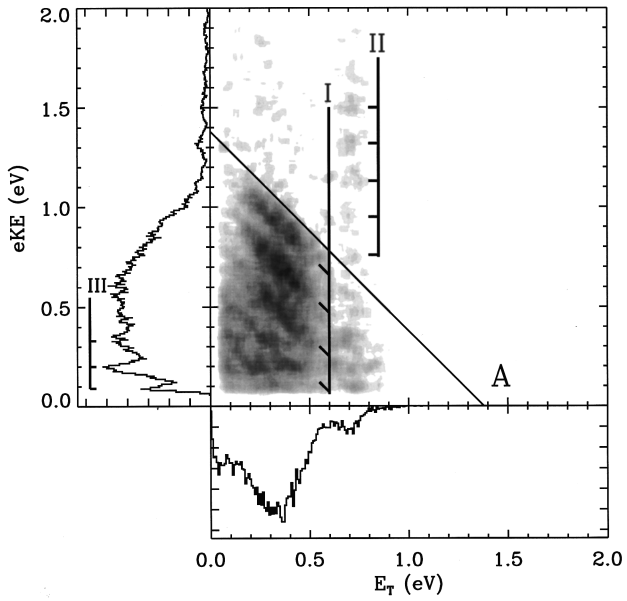

FIG. 2. $N(\text{eKE}, E_T)$ correlation spectrum for O_6^- at 532 nm. The energetic limit *A* for the process $O_6^- + h\nu \rightarrow O_2(X\ ^3\Sigma_g^-) + O_2(X\ ^3\Sigma_g^-) + O_2(X\ ^3\Sigma_g^-) + e^-$ is shown. The contours are linearly scaled and the marked features are discussed in the text.

by I. These ridges are very similar to the features previously observed in the DPD of O_4^- at 532 nm.[16] In the DPD of O_4^-, a series of five diagonal ridges were observed in the photoelectron–photofragment correlation spectrum, corresponding to direct DPD on a series of vibrationally adiabatic repulsive curves correlating to ground electronic state $O_2(v=0)+O_2(v=0)$, $O_2(v=0)+O_2(v=1)$, and so forth. In the O_6^- spectrum, these diagonal bands are shifted to a lower eKE and E_T, due to the 0.11 eV stability of O_6^- relative to $O_4^-+O_2$.[15] In the correlation spectrum, internal energy of the photofragments appears as a displacement along the diagonal between the origin and the limit *A*. The separation of the ridges along the diagonal is ≈0.19 eV, consistent with the vibrational spacing of the O_2 photofragments. Thus, as in the case of O_4^-, these features are assigned to the correlated product state distribution of the O_2 products.

These diagonal features in the correlation spectrum arise from direct DPD of a bound anion on a repulsive electronic state of the nascent neutral complex. The eKE is determined by the photon energy and the vertical energy difference between anion and neutral, while E_T for a given DPD event contains additional information concerning the repulsive energy in the neutral complex relative to the dissociation asymptote. Energy conservation dictates that all events that lie within a single ridge have a well-defined total kinetic energy ($E_{\mathrm{tot}}=\mathrm{eKE}+E_T$). Within a given ridge, however, there is a range of energy partitioning between the electron and photofragments that is determined by the Franck–Condon overlap between a bound coordinate in the anion and the dissociation coordinate.

There are two other important features in Fig. 2. Feature II, the vertical row of spots at $E_T=0.7$ eV, results from a photodissociation process $O_6^-+h\nu\rightarrow O_2(^1\Delta_g,v=0)+O_2^-(^2\Pi_g,v=0)+O_2(^3\Sigma_g^-)$. The analogous process $O_4^-+h\nu\rightarrow O_2(^1\Delta_g,v=0)+O_2^-(^2\Pi_g,v=0)$ was previously observed, at an $E_T=0.8$ eV. The lower E_T observed in the photodissociation of O_6^- is consistent with the 0.11 eV stability of O_6^- relative to $O_4^-+O_2$. These features are observable in this experiment (that only detects neutral photofragments) due to photodetachment of the nascent $O_2^-(v=0)$ photofragments by a second photon, yielding the well-known photoelectron spectrum of $O_2^-(v=0)$[13,23] as the vertical row of spots. Finally, feature III is a second photodissociation process, not observed in O_4^- at 532 nm; $O_6^-+h\nu\rightarrow O_2^-(^2\Pi_g,v>3)+O_2(^3\Sigma_g^-)+O_2(^3\Sigma_g^-)$. The peaks visible in the photoelectron spectrum appear at energies of 0.09, 0.19, and 0.30 eV, consistent with autodetachment of $O_2^-(v=4,5,6)\rightarrow O_2(v=0)+e^-$. Observation of maximum Δv autodetachment of O_2^- was discussed by Schultz and co-workers,[24] and is thought to derive from the high centrifugal barrier faced by the autodetaching $l=2$ *d*-wave photoelectron. Higher-resolution photoelectron spectra from this laboratory have shown that the peak for $O_2^-(v=7)$ autodetachment is also observed at 0.41 eV.[25] A consideration of the energetics indicates that this process can only occur if no $O_2(^1\Delta_g)$ is produced in this photodissociation channel.

In Fig. 3 the E_{tot} spectra for O_4^- (from Ref. 16) and O_6^- are shown in the lower and upper frames, respectively. These spectra are generated from the correlation spectra by histogramming $E_{\mathrm{tot}}=\mathrm{eKE}+E_T$ for each event. The shift of the threshold *A* in the O_6^- spectrum is due to the stability of O_6^- relative to $O_4^-+O_2$. The diagonal ridges of Fig. 2 now appear as resolved peaks in the O_6^- data. The spectrum shows that the DPD of O_6^- is characterized by an increase in the relative intensities of the peaks corresponding to vibrationally excited O_2 relative to O_4^-. There is also evidence of increased rotational excitation at higher vibrational energies, as shown by the shift of the peaks and reduction in resolution at lower E_{tot}. The fact that these peaks are resolved indicates that the rotational distribution in the photofragments, even in the case of O_6^-, is narrow and generally less than a vibrational quantum. Remarkably, the dynamics observed in DPD of O_4^- are largely preserved in O_6^-.

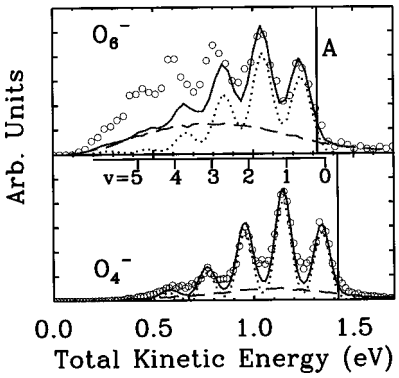

FIG. 3. Total kinetic energy (E_{tot}) spectra for DPD of O_4^- and O_6^- are shown in the lower and upper frames, respectively. The energetic limit *A* for O_6^- is the same as in Fig. 2. The spacing of the first five vibrational levels of O_2 are shown in the lower frame for reference. The circles represent the data, and the solid line represents the sum of the contributions from the local-mode Franck–Condon fit (dotted-line curve) and a background contribution generated from the random correlation of the eKE and E_T spectra (dashed-line curve).

The low observed rotational excitation indicates that, like O_4^-, there is a restricted range of product angular momenta produced in the dissociation of the nascent O_6 neutral. This result is consistent with either a weakly bound ion–dipole complex, in which the third O_2 is merely a spectator, or perhaps a molecular O_6^- anion with a reasonably high symmetry. The observed product vibrational distribution is not consistent with either extreme limit, however, at least within the framework of the simple local-mode Franck–Condon simulation previously used in the analysis of the O_4^- E_{tot} spectrum. In this calculation, the probability for each energetically allowed combination of vibrational states is calculated as a product of the individual diatom Franck–Condon factors, taking into account the degeneracy for a given set of product vibrational states. A good fit to the O_4^- E_{tot} spectrum, shown by the solid line in Fig. 3, was generated by calculating the overlap of the vibrational wave functions of two perturbed O_2 moieties ($r_e=1.272$ Å, $\omega_e=1335$ cm^{-1}) with two free O_2 ($^3\Sigma_g^-$) molecules. In the limit of a weak interaction between O_2 and O_4^-, a similar distribution would be expected for O_6^-. An examination of Fig. 3 shows that the O_4^- distribution predicts lower vibrational excitation than observed in O_6^-. An alternative possibility for O_6^- is that all three short O–O bonds are equal,

with $r_e = 1.255$ Å, one third of the difference between O_2 and O_2^-. This fit, shown on the O_6^- spectrum, does not reproduce the correlated product vibrational distribution. A better fit to the data will require more information on the structure of O_6^- and the dynamics of the three-body dissociation of O_6.

In conclusion, we report the first complete kinematic description of a three-body DPD process. These results show that while the DPD dynamics of O_6^- are remarkably similar to O_4^-, a more marked change is observed in the photodissociation dynamics. The low rotational excitation in the products permits the observation of vibrationally resolved translational energy distributions and argues for either an O_4^- core bound electrostatically to a third O_2 or perhaps, a highly symmetric structure for O_6^-. Studies of the photodestruction dynamics at other wavelengths and theoretical calculations of the O_6^- structure are under way to resolve this question. In future studies, the time scale for three-body dissociation will be addressed by examination of the photoelectron–photofragment and photofragment–photofragment angular correlations, and this technique will be extended to important systems including the three-body association reaction responsible for the formation of ozone: $O+O_2+M \rightarrow O_3+M$.

Support by the Air Force Office of Scientific Research under Grant No. F49620-96-1-0220 is acknowledged. A.K.L. is supported by an AFOSR AASERT Grant No. F49620-97-1-0387. R.E.C. is a Camille Dreyfus Teacher-Scholar, an Alfred P. Sloan Research Fellow, and a David and Lucile Packard Fellow in Science and Engineering.

[1] Recent experiments on three-body dissociation are extensively reviewed in: C. Maul and K. H. Gericke, Int. Rev. Phys. Chem. **16**, 1 (1997).
[2] W. H. Miller, J. Phys. Chem. **99**, 12387 (1995); R. J. Duchovic, J. D. Pettigrew, B. Welling, and T. Shipchandler, J. Chem. Phys. **105**, 10367 (1996); A. Gross and G. D. Billing, Chem. Phys. **217**, 1 (1997); R. T Pack, R. B. Walker, and B. Kendrick, J. Chem. Phys (in press).
[3] J. H. D. Eland, in *VUV Photoionization and Photodissociation of Molecules and Clusters*, edited by C. Y. Ng (World Scientific, Singapore, 1991), pp. 297–343.
[4] U. Werner, K. Beckord, J. Becker, and H. O. Lutz, Phys. Rev. Lett. **74**, 1962 (1995).
[5] T. Masuoka, J. Chem. Phys. **98**, 6989 (1993).
[6] P. M. Kroger and S. J. Riley, J. Chem. Phys. **67**, 4483 (1977).
[7] X. Zhao, W. B. Miller, E. J. Hintsa, and Y. T. Lee, J. Chem. Phys. **90**, 5527 (1989).
[8] C. E. M. Strauss and P. L. Houston, J. Phys. Chem. **94**, 8751 (1990).
[9] T. Gejo, J. A. Harrison, and J. R. Huber, J. Phys. Chem. **100**, 13941 (1996).
[10] S. W. North, A. J. Marr, A. Furlan, and G. E. Hall, J. Phys. Chem. A **101**, 9224 (1997).
[11] D. Stranges, X. Yang, J. D. Chesko, and A. G. Suits, J. Chem. Phys. **102**, 6067 (1995).
[12] R. E. Continetti, Int. Rev. Phys. Chem. **17**, 227 (1998).
[13] M. J. Deluca, C. C. Han, and M. A. Johnson, J. Chem. Phys. **93**, 268 (1990); C. C. Han and M. A. Johnson, Chem. Phys. Lett. **189**, 460 (1992).
[14] C. R. Sherwood, K. A. Hanold, M. C. Garner, K. M. Strong, and R. E. Continetti, J. Chem. Phys. **105**, 10803 (1996).
[15] K. Hiraoka, J. Phys. Chem. **89**, 3190 (1988).
[16] K. A. Hanold, M. C. Garner, and R. E. Continetti, Phys. Rev. Lett. **77**, 3335 (1996).
[17] K. A. Hanold and R. E. Continetti, Chem. Phys. (in press).
[18] G. V. Chertihin and L. Andrews, J. Chem. Phys. **108**, 6404 (1998).
[19] K. A. Hanold, A. K. Luong, and R. E. Continetti, Rev. Sci. Instrum. (submitted).
[20] X. Xie and J. D. Simon, Opt. Commun. **69**, 303 (1989).
[21] M. Lampton, O. Siegmund, and R. Raffanti, Rev. Sci. Instrum. **58**, 2298 (1987).
[22] P. G. Friedman, R. A. Cuza, J. R. Fleischman, C. Martin, D. Schiminovich, and D. J. Doyle, Rev. Sci. Instrum. **67**, 596 (1996).
[23] M. J. Travers, D. C. Cowles, and G. B. Ellison, Chem. Phys. Lett. **164**, 449 (1989).
[24] G. J. Schulz, Rev. Mod. Phys. **45**, 423 (1973).
[25] R. Li, K. A. Hanold, M. C. Garner, A. K. Luong, and R. E. Continetti, Faraday Discuss. **108**, 115 (1997).